

# ***N*<sup>6</sup>-Methyladenosine modification of lincRNA 1281 is critically required for mESC differentiation potential**

**Dandan Yang, Jing Qiao, Guiying Wang, Yuanyuan Lan, Guoping Li, Xudong Guo, Jiajie Xi, Dan Ye, Songcheng Zhu, Wen Chen, Wenwen Jia, Ye Leng, Xiaoping Wan and Jihong Kang\***

Clinical and Translational Research Center of Shanghai First Maternity and Infant Health Hospital, Shanghai Key Laboratory of Signaling and Disease Research, Collaborative Innovation Center for Brain Science, School of Life Sciences and Technology, Tongji University, 1239 Siping Road, Shanghai 200092, China

Received June 16, 2017; Revised February 10, 2018; Editorial Decision February 13, 2018; Accepted February 13, 2018

## **ABSTRACT**

**Previous studies have revealed the critical roles of *N*<sup>6</sup>-methyladenosine (*m*<sup>6</sup>A) modification of mRNA in embryonic stem cells (ESCs), but the biological function of *m*<sup>6</sup>A in large intergenic noncoding RNA (lincRNA) is unknown. Here, we showed that the internal *m*<sup>6</sup>A modification of *linc1281* mediates a competing endogenous RNA (ceRNA) model to regulate mouse ESC (mESC) differentiation. We demonstrated that loss of *linc1281* compromises mESC differentiation and that *m*<sup>6</sup>A is highly enriched within *linc1281* transcripts. *Linc1281* with RRACU *m*<sup>6</sup>A sequence motifs, but not an *m*<sup>6</sup>A-deficient mutant, restored the phenotype in *linc1281*-depleted mESCs. Mechanistic analyses revealed that *linc1281* ensures mESC identity by sequestering pluripotency-related let-7 family microRNAs (miRNAs), and this RNA-RNA interaction is *m*<sup>6</sup>A dependent. Collectively, these findings elucidated the functional roles of *linc1281* and its *m*<sup>6</sup>A modification in mESCs and identified a novel RNA regulatory mechanism, providing a basis for further exploration of broad RNA epigenetic regulatory patterns.**

## **INTRODUCTION**

Embryonic stem cells (ESCs) have two defining features: the ability of self-renewal and the capacity to give rise to most cell types. These unique features of ESCs have made them a valuable tool for clinical therapies and enabled the *in vitro* study of early mammalian development. Multiple genes, including transcription factors, chromatin-remodeling enzymes and signaling molecules, are precisely coordinated to control ESC pluripotency (1,2). In addition to protein-coding genes, large intergenic noncoding RNAs (lincRNAs)

are a novel class of gene regulators that function as signals, scaffolds, molecular decoys and mediators of long-range chromatin interactions (3). ESC-specific lincRNAs have been identified using the chromatin signature of actively transcribed genes (4,5). Researchers recently demonstrated that the vast majority of these lincRNAs are required for the maintenance of ESC pluripotency by performing systematic loss-of-function experiments, which indicated that lincRNAs are involved in the molecular circuitry of ESCs (6). However, relatively little is known about the functional role of individual lincRNAs in ESCs, and it remains unclear how lincRNAs epigenetically modulate ESC self-renewal and cell-fate decisions. Characterization of lincRNA pathways and their underlying molecular mechanisms is therefore important for understanding ESC pluripotency.

Analysis of the role of RNA modification in the regulation of gene expression has led to the development of the new field of ‘RNA epigenetics’ (7). *N*<sup>6</sup>-methyladenosine (*m*<sup>6</sup>A) is the most abundant internal RNA modification in mammalian systems (8) and plays a diverse role in epigenetic regulation of RNA metabolism, including mRNA stability (9,10), alternative splicing (11,12), cap-independent protein translation (13) and microRNA (miRNA) biogenesis (14). *m*<sup>6</sup>A biology is crucial for cell status regulation, sex determination and development (12,15–23). Dysregulation of this modification is clearly linked to human diseases such as obesity and cancer (24). Recent studies have suggested the involvement of *m*<sup>6</sup>A in mouse ESC (mESC) self-renewal and cell-fate decisions (10,25,26). Genetic inactivation or deletion of *Mettl3* (an RNA methyltransferase complex component) in mESCs, and hence *m*<sup>6</sup>A, blocked differentiation and resulted in early embryonic lethality. To elucidate the function and regulatory mechanism of *m*<sup>6</sup>A in mESCs, researchers identified a large number of core pluripotency regulators in mESCs, such as *Nanog*, *Klf4*, *Med1* and *Eed*, showing *m*<sup>6</sup>A modifications. The *m*<sup>6</sup>A mark impairs the stability of methylated transcripts in mESCs

\*To whom correspondence should be addressed. Tel: +86 21 65988876; Fax: +86 21 65981041; Email: jhkang@tongji.edu.cn

by increasing mRNA degradation rates. In the absence of m<sup>6</sup>A modification, mESCs show prolonged Nanog expression upon differentiation, which inhibits the exit of mESCs from self-renewal. All studies performed on this topic to date have addressed the critical role of the m<sup>6</sup>A modification of mRNA in the RNA methylation-mediated control of stemness. However, no reports have addressed the biological function of m<sup>6</sup>A in lincRNAs, despite the fact that some mESC-expressed lincRNAs are m<sup>6</sup>A modified (26), and lincRNAs are key players in the mESC pluripotency regulatory circuit. We therefore hypothesize that m<sup>6</sup>A in lincRNAs may mediate the relationship between lincRNAs and transcriptional networks in mESCs.

As key posttranscriptional modifiers, miRNAs have been shown to be involved in maintaining mESC pluripotency. mESCs with genetic deletion of the miRNA processing enzyme Dicer or DGCR8 exhibit differentiation-defective phenotypes (27–29). A number of studies have identified mESC-specific miRNAs and have shown that miRNAs are key regulators of mESC self-renewal and cell fate decisions (30–33). MiRNAs modulate the pluripotent state by fine tuning the expression of target genes, including mESC-specific transcription factors and key pathway molecules. However, although miRNA-mediated pathways in mESCs have been extensively characterized, the regulatory networks modulating miRNA function have not been fully elucidated. Recently, several authors have proposed a lincRNA-mediated regulatory model in which lincRNA functions as competing endogenous RNA (ceRNA) to modulate the activities and biological functions of miRNAs. These reports have indicated that linc-MD1 acts as a sponge of miR-133 and miR-135 to protect the mRNA of the muscle-specific genes MAML1 and MEF2C (34). Human pluripotency-associated transcript 5 (HPAT5) binds directly with the let-7 miRNA family to modulate reprogramming and human ESC (hESC) differentiation (35). Linc-RoR has also been identified as a ceRNA that sequesters differentiation-related miRNAs in hESCs and regulates the expression of the core transcription factors OCT4, SOX2 and NANOG (36). These studies suggested that ceRNA-mediated crosstalk plays a critical role in the ‘RNA epigenetics’ network controlling ESC stemness. The characterization of this RNA-RNA interaction in ESCs is important for our understanding of the regulation of ESC pluripotency and RNA functions.

Here, we first elucidated the functional role of m<sup>6</sup>A modification of lincRNA in the regulation of mESC pluripotency. We found that the mESC-specific *linc1281* is necessary for mESC differentiation, and its essential functional role relies on m<sup>6</sup>A enrichment within the last exon of *linc1281*.

## MATERIALS AND METHODS

### Cell culture and differentiation

Sox1-GFP mouse ES cells (37) (46C; a gift from A. Smith) were maintained on feeders under mESC culture conditions. For embryoid body (EB) differentiation, mESCs were plated at a density of  $5 \times 10^4$  cells/ml in ultra-low-attachment plates in mESC medium without LIF. The medium was changed every two days, and on day 4, the

EBs were seeded onto a gelatin-coated 48-well plate. For neural differentiation, the mESCs were grown in differentiation medium (G-MEM supplemented with 8% Knockout Serum Replacement, 2 mM glutamine, 1 mM sodium pyruvate, 0.1 mM non-essential amino acids and 0.1 mM 2-mercaptoethanol with or without 5% FBS). For quantification of the percentage of Sox1<sup>+</sup> cells, mESCs were dissociated into single cells in 0.25% trypsin-EDTA, and FACS analysis was immediately performed.

### CRISPR-mediated *linc1281* knockout

Plasmids for guide RNA (designed with the CRISPR design tool Zinc Finger Targeter (38,39)), a Cas9 expression plasmid, and a donor plasmid containing the PGK-Puro insert were cotransfected into mESCs using an electroporation method. Cells were plated at low density and treated with puromycin two days after transfection. Single colonies were selected and tested for loss of *linc1281*.

### Lentiviral vectors

For the generation of shlinc1281 or shMettl3, short hairpin RNAs targeting *linc1281* or *Mettl3*-specific regions (shlinc1281-1, ACGGAGATACAAGACCATTG; shlinc1281-2, GGTTCTTCTTGGCCCTATTAA; shMettl3-1, GCACACTGATGAATCTTTA; shMettl3-2, CGTCAGTATCTTGGGCAAATT) were designed and cloned into the pLKO.1-TRC cloning vector. The full-length *linc1281* (NC\_000079.6) was synthesized and cloned into the FUGW vector to generate an overexpression vector. Mutations were generated using the QuikChange Lightning Multi Site-Directed Mutagenesis Kit (Agilent Technologies).

### qRT-PCR analysis

Total RNA was extracted using the RNAiso Reagent (TaKaRa) according to the manufacturer’s instructions. The synthesis of cDNA was performed using the PrimeScript RT reagent kit (TaKaRa). qRT-PCR analysis was performed using the SYBR Green qPCR Master Mix (Bio-Rad). MiRNA levels were measured using the Bulge-Loop™ miRNA qPCR Primer Set (RiboBio) according to the manufacturer’s instructions.

### Immunofluorescence staining

For immunofluorescence staining, cells were washed with PBS, fixed with 4% paraformaldehyde for 20 min and then permeabilized with 0.2% Triton X-100 for 8 min. The cells were then washed twice with PBS, blocked in 10% FBS for 45 min and incubated overnight with primary antibodies at 4°C. Next, the cells were stained with fluorescent secondary antibodies for 2 h and with Hoechst 33342 dye for 20 min. Images were acquired using a fluorescence microscope. The primary antibodies used in this work included anti-cTnT (Abcam), anti-N-cad (BD) and anti-GFP (Abcam).

### Western blotting

Cells were collected, washed twice with ice-cold PBS and incubated on ice for 30 min with RIPA lysis buffer (Beyotime). Protein concentrations were measured using the Pierce BCA Protein Assay Kit (Thermo). Primary antibodies including anti-Lin28a (Cell Signaling Technology), anti-Lin28b (Cell Signaling Technology), anti-Mettl3 (Abcam) and anti-GAPDH (Bioworld Technology) were used in these assays.

### RNA FISH

For the detection of *linc1281*, RNA FISH was conducted using a Fluorescent in Situ Hybridization Kit (RiboBio) in accordance with the manufacturer's directions. The probe mix used for *linc1281* was lnc1100439 (RiboBio).

### Cytoplasmic and nuclear RNA fractionation

Nuclear and cytoplasmic RNA was isolated as previously described (40). mESCs were collected, washed twice with ice-cold PBS and centrifuged at 1000 rpm for 10 min. Cell pellets were gently resuspended and incubated on ice for 5 min in 200  $\mu$ l of lysis buffer A [Tris (10 mM, pH 8.0), NaCl (140 mM), MgCl<sub>2</sub> (1.5 mM) 0.5% Nonidet P-40] and then centrifuged at 1000  $\times$  g for 3 min at 4°C. The supernatant, containing the cytoplasmic fraction, was added to 1 mL of RNAiso Reagent. Nuclear pellets were washed with lysis buffer A twice, followed by washing with lysis buffer A containing 1% Tween-40 and 0.5% deoxycholic acid, and then resuspended in 1 ml of RNAiso Reagent. Purification and analysis of cytoplasmic and nuclear RNA were subsequently performed via qRT-PCR assays.

### RIP assay

The MS2bp-MS2bs-based RIP assay was performed as described previously (40). HEK293FT cells were cotransfected with 8  $\mu$ g of the MS2bs-*linc1281* vector or the blank control vector MS2bs-*Renilla*, 8  $\mu$ g of the MS2bp-YFP plasmid and miRNA mimics (50 nM), using 100  $\mu$ l of FuGENE HD reagent (Roche). After 48 h, the cells were collected and subsequently lysed with lysis buffer [KCl (100 mM), MgCl<sub>2</sub> (5 mM), HEPES (10 mM, pH 7.0), NP-40 (0.5% v/v), DTT (1 mM), PI (100 $\times$ ), RNaseOut (0.1 U/ $\mu$ l), PMSF (1 mM)] for 30 min on ice. Immunoprecipitation was performed using anti-YFP (Abcam) or control rabbit IgG (Cell Signaling Technology). The RNA complexes were isolated through phenol-chloroform extraction and analyzed via qRT-PCR assays.

### Biotin-RNA pull-down and LC-MS

To identify *linc1281*-interacting proteins in mESCs, biotin-RNA pull down and subsequent liquid chromatography-mass spectrometry were performed. Briefly, biotin-labeled RNAs were synthesized by using RNA Labeling Mix (Roche, 11685597910) and T3/T7 RNA polymerase (Roche, 10881767001/11031171001). *Linc1281* or antisense RNAs were heated to 90°C for 2 min, held on ice for 2 min and then incubated in room temperature for 20 min in

RNA structure buffer (10 mM Tris-HCl pH 7.0, 0.1 M KCl and 10 mM MgCl<sub>2</sub>) to form proper secondary structure. mESCs ( $1 \times 10^7$  cells) were lysed with RIP lysis buffer and Immunoprecipitation was performed by using streptavidin beads coated with 3  $\mu$ g of *linc1281* or antisense RNAs. The RNA-binding proteins were sequenced and identified by LC-MS as described previously (41). The mass spectra were searched using the Mascot Daemon software (Version 2.3.0, Matrix Science, London, UK) based on the Mascot algorithm. The database used to search was the Mouse UniProtKB database.

### Measurement of m<sup>6</sup>A-modified *linc1281* levels

For quantification of m<sup>6</sup>A-modified *linc1281* levels, methylated RNA immunoprecipitation was performed. A 1.5  $\mu$ g aliquot of anti-m<sup>6</sup>A antibody (Synaptic Systems, 202003) or anti-IgG (Cell Signaling Technology) was conjugated to protein A/G magnetic beads overnight at 4°C. A 100  $\mu$ g aliquot of total RNA was then incubated with the antibody in IP buffer supplemented with RNase inhibitor and protease inhibitor. RNA was eluted with elution buffer, purified through phenol-chloroform extraction and then analyzed via qRT-PCR assays.

### Dual-luciferase assay

Luciferase reporters were generated by cloning *linc1281* or mutant *linc1281* into pGL3-basic vectors. Mutant vectors were obtained using the QuikChange Lightning Multi Site-Directed Mutagenesis Kit (Agilent Technologies). Then, NIH/3T3 cells ( $3 \times 10^4$ ) were cotransfected with 100 ng of reporter, 5 ng of the internal control Renilla vector and miRNA mimics (50 mM), with 1  $\mu$ l of the FuGENE HD reagent. Cell lysates were harvested 48 hr after transfection, and luciferase activities were examined using the Dual-Luciferase Reporter Assay System (Promega).

### Teratoma generation

mESCs were trypsinized into single cells, resuspended at a concentration of  $1.5 \times 10^6$  cells/150  $\mu$ l and then injected into athymic nude mice (NOD-SCID) obtained from the National Resource Center of Mutant Mouse Model Animal Research Center (NARC), NJU. Tumors were assessed every week and harvested 4 weeks later. All experiments were carried out as approved by the Institutional Animal Care and Use Committee of Tongji University.

### Statistical analysis

Statistical significance was analyzed with Student's *t*-test (two-tailed). The error bar represents the standard error of the mean (SEM), and all experiments were independently repeated at least three times.

## RESULTS

### *Linc1281* is required for proper mESC differentiation

To explore the functions of *linc1281* in mESCs, we analyzed *linc1281* levels of mESCs in the presence or absence

of LIF for 4 days via qRT-PCR. *Linc1281* was significantly enriched in mESCs, suggesting its association with pluripotency (Figure 1A). RNA FISH assays and analysis of the cellular distribution of RNAs both showed that *linc1281* transcripts were abundant in the cytoplasm of mESCs (Figure 1B and C). Thus, we performed shRNA-mediated loss-of-function assays, in which two distinct shRNAs resulted in at least 85% knockdown of endogenous *linc1281* in mESCs (Figure 1D). *Linc1281*-depleted cells exhibited normal properties of self-renewal, with no change in the expression levels of mESC-specific genes, including *Oct4*, *Sox2* and *Nanog*, suggesting that *linc1281* is dispensable for mESC self-renewal and may be involved in other aspects of stem cell biology (Figure 1E). We next examined whether the differentiation capacity of mESCs was affected when *linc1281* expression was reduced *in vivo*. We subcutaneously injected *linc1281*-depleted or control cells into immune-deficient mice. Although both cell types formed tumors with morphology consistent with teratomas, the tumors derived from *linc1281*-depleted cells were significantly smaller and lower in weight than control tumors (Figure 1F). Histological analysis of hematoxylin and eosin (H&E)-stained tumor sections revealed that teratomas derived from *linc1281*-deficient cells contained few structures from all three germ layers (Figure 1G). The decreased expression of lineage-specific markers in tumors from *linc1281*-deficient cells further confirmed that differentiation was disrupted in *linc1281*-depleted mESCs (Figure 1H).

Next, we tested the *in vitro* capacity for directed differentiation toward two lineages: mesoderm-derived cardiomyocytes and ectoderm-derived neural lineage cells, which are two ideal *in vitro* differentiation models for analysis of the mechanisms underlying the developmental process. qRT-PCR analysis showed that in the reduction by knockdown of *linc1281*, mESCs displayed significantly reduced expression levels of mesoderm (*Gata4*, *Mesp1* and *Cxcr4*), cardiac progenitor (*Mef2c*, *Isl1* and *Tbx5*) and cardiomyocyte marker genes (*Myl2*, *Myh6*, *Myl7*, *Slc8a1*, *MHC* and *cTnT*) (Figure 1I). While 75% (EB Day 10) or 80% (EB Day 12) of EBs generated from control cells could differentiate into spontaneously beating cardiomyocytes, only 40% (EB Day 10) or 50% (EB Day 12) of *linc1281*-deficient EBs developed spontaneously into contracting clusters (Figure 1J). Immunostaining showed that differentiated EBs from *linc1281*-deficient cells had reduced expression of cTnT (Figure 1K). Similarly, compared with control cells, *linc1281*-deficient cells showed decreased differentiation into the neural lineage: the cells exhibited a substantially reduced percentage of Sox1 (a neural-progenitor-specific gene)-positive (Sox1<sup>+</sup>) cells (Figure 1L), lower expression levels of neural markers (*Sox1*, *Pax6*, *N-cad*, *Zfp521*, *Map2* and *Tuj1*, Figure 1M) and a decrease in Sox1-GFP/*N-cad*-positive cells (Figure 1N). To further address the functions of *linc1281* in maintaining mESC pluripotency, we targeted *linc1281* via CRISPR-mediated gene editing and generated *linc1281* knockout (KO) mESC lines (Supplementary Figure S1A and B). RNA FISH and qRT-PCR analyses confirmed the absence of *linc1281* (Supplementary Figure S1C-D). Consistent with the results from the shRNA-mediated loss-of-function assays, *linc1281* KO cells showed no significant differences in the expression levels of pluripotency

markers (*Oct4*, *Sox2* and *Nanog*) and a reduced capacity for differentiation (Supplementary Figure S1E-M). Furthermore, the forced expression of *linc1281* significantly enhanced mESC differentiation, while showed no effect on the expression levels of mESC-specific genes (Supplementary Figure S2A and B). In EB formation assays, mESCs overexpressing *linc1281* showed increases in the expression levels of lineage markers, the percentages of EBs containing spontaneously beating areas and cTnT-positive cell numbers (Supplementary Figure S2C-G). In neural differentiation assays, the forced expression of *linc1281* enhanced the efficiency of neural generation in nonpermissive cultures containing 5% FBS (Supplementary Figure S2H-J). Furthermore, we precisely evaluated the physiological levels of *linc1281* in mESCs and differentiated cell populations from mESCs and found that *linc1281* showed quite low expression in differentiated cells compared with that in mESCs, which was consistent with the above observation (Supplementary Figure S3). Considering all of these findings together, we concluded that depletion of *linc1281* in mESCs inhibits their capacity for differentiation and that *linc1281* is required for proper differentiation of mESCs.

### The m<sup>6</sup>A modification is enriched in *linc1281*

Recent studies have suggested that the m<sup>6</sup>A RNA modification can determine the fate of mESCs, and thousands of mESC-specific transcripts, including lincRNAs, are modified by m<sup>6</sup>A. We investigated the m<sup>6</sup>A modification of *linc1281* in mESCs because this lincRNA is a critical regulator of differentiation in mESCs and may be modified by m<sup>6</sup>A according to a previous report (26). We verified the m<sup>6</sup>A modification of *linc1281* by performing a methylated RNA immunoprecipitation (MeRIP) assay (Figure 2A). To further characterize the m<sup>6</sup>A methylation of *linc1281*, we performed shRNA-mediated downregulation of *Mettl3*, an important component of the m<sup>6</sup>A methylase complex, in mESCs. The sh*Mettl3* cell lines exhibited 70% knockdown of the endogenous *Mettl3* protein and RNA and no change in the expression levels of *linc1281* (Figure 2B and C). Nevertheless, *Mettl3* deficiency substantially decreased the m<sup>6</sup>A level on *linc1281*, indicating that *Mettl3* is a major m<sup>6</sup>A methylase for *linc1281* in mESCs (Figure 2D).

### The internal m<sup>6</sup>A mark is positively involved in the functional role of *linc1281* in mESCs

The *linc1281* RNA molecule contains 1306 nucleotides and is generated from 3 exons. To further define the potential functions of m<sup>6</sup>A-modified *linc1281*, we analyzed the m<sup>6</sup>A sites located in *linc1281* and found three RRACU m<sup>6</sup>A sequence motifs in the last exon, which was previously described as a location for m<sup>6</sup>A deposition (Figure 2E). Next, we constructed expression vectors harboring *linc1281* point mutants, in which the adenine residues embedded within the m<sup>6</sup>A motifs were replaced with guanine (A-G transition mutation) or thymine (A-T transversion mutation), and a deletion mutant, in which the adenine residues were deleted. The mutants in which with a single (A<sup>916</sup>-G) or three (A<sup>916, 1024 and 1054</sup>-G) unmethylated adenine residues within the m<sup>6</sup>A motifs were replaced with guanine were employed as controls. We transfected HEK293FT cells, which

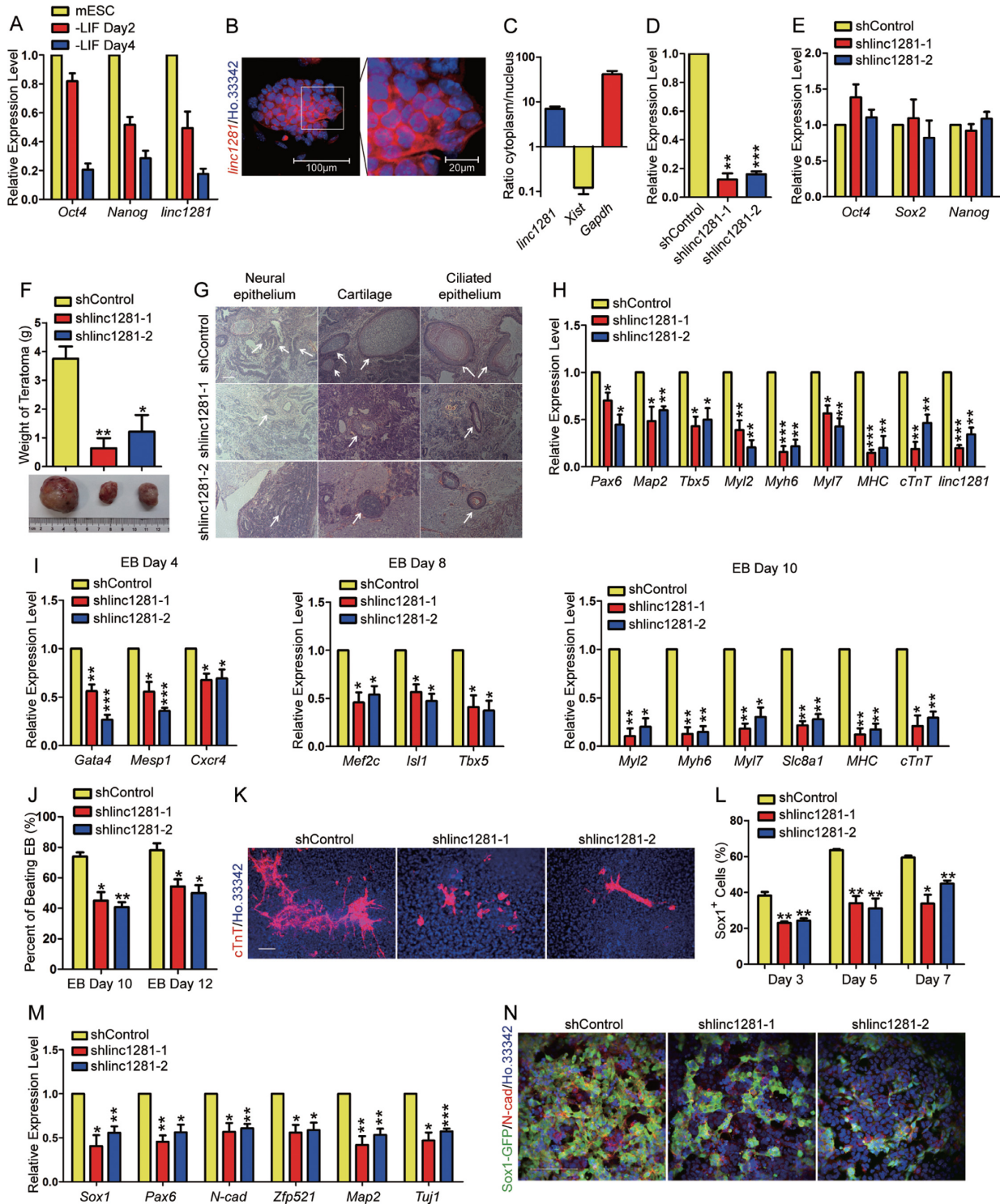


**Figure 1.** *Linc1281* is required for proper mESC differentiation. (A) Expression levels of *linc1281* in mESCs in the presence or absence LIF for 4 days. (B) RNA FISH for *linc1281* in mESCs. Scale bar represents 100 or 20 μm. (C) qRT-PCR analysis of transcripts derived from the cytoplasmic or nuclear fractions of mESCs. The log<sub>10</sub> ratio of cytoplasmic to nuclear transcripts is presented. (D) qRT-PCR analysis of *linc1281* knockdown efficiency. pLKO.1-scramble shRNA was used as a negative control. (E) mRNA levels of *Oct4*, *Sox2* and *Nanog* upon *linc1281* depletion determined via qRT-PCR. (F) Weight differences between teratomas generated from shControl and shlinc1281 cells. (G) Representative sections of teratomas stained with H&E. Scale bar represents 25 μm. (H) Lineage-specific marker expression in teratomas. (I) qRT-PCR analysis of mesoderm (left), cardiac progenitor (middle) and cardiomyocyte markers (right) during EB formation. EB, embryoid bodies. (J) Percentage of EBs with beating activity. (K) Representative images of bodies stained for cTnT and Hoechst 33342 (Ho.33342) on day 12 of EB formation. Scale bar represents 100 μm. (L) Percentage of Sox1<sup>+</sup> cells analyzed via FACS during neural lineage differentiation. (M) qRT-PCR analysis of neural markers on day 5 of neural differentiation. (N) Representative images of cells stained for Sox1-GFP, N-cad and Ho.33342 on day 5 of neural differentiation. Scale bar represents 100 μm. Error bars show ± SEM ( $n \geq 3$ ). \*\*\* $P < 0.001$ , \*\* $P < 0.01$ , \* $P < 0.05$  versus shControl.

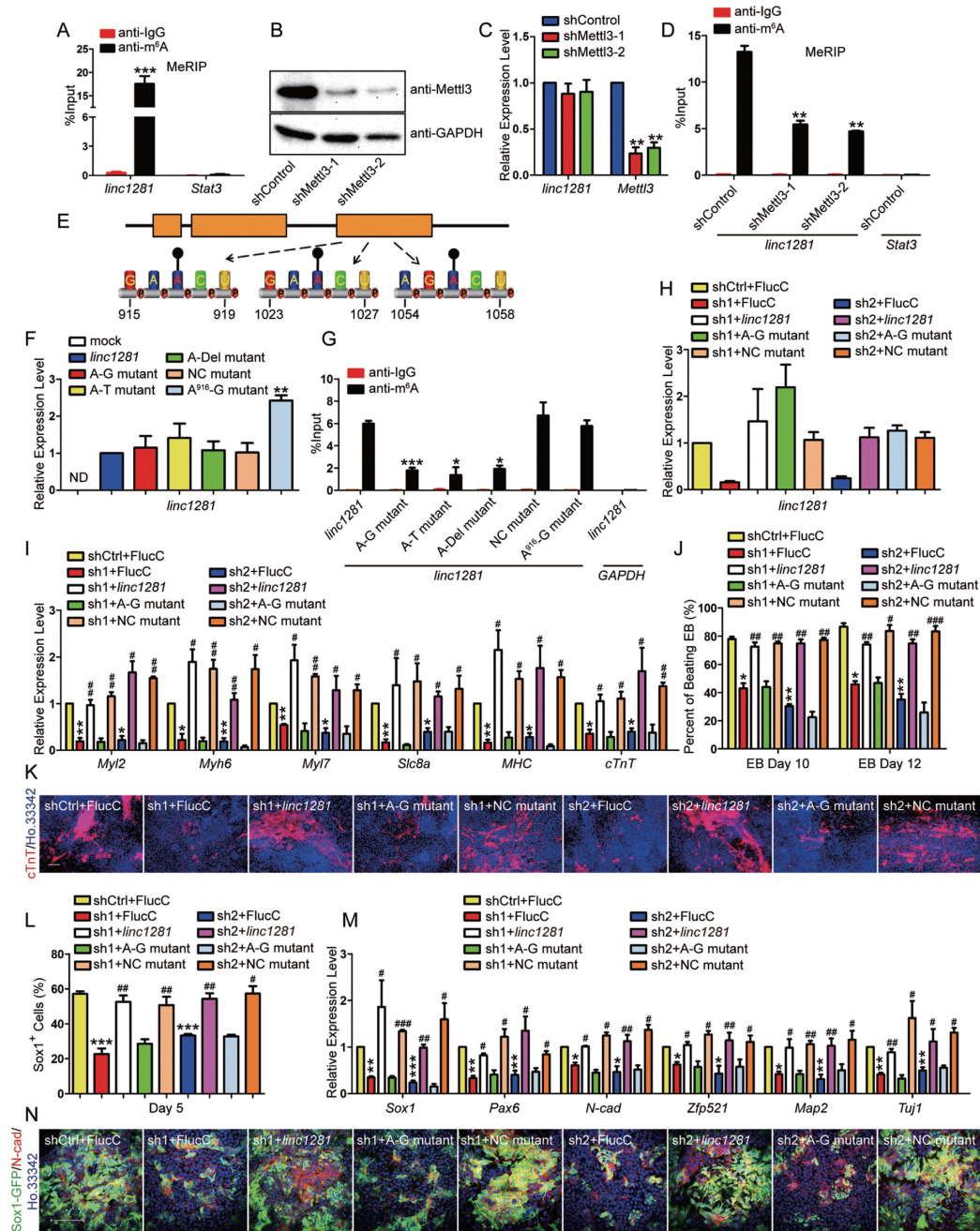


**Figure 2.** m<sup>6</sup>A enrichment is positively associated with the role of *linc1281* in mESCs. (A) Enrichment of m<sup>6</sup>A-modified *linc1281* in mESCs. Unmethylated transcript *Stat3* was used as negative control. The percentage of the input is shown. Error bars show  $\pm$  SEM ( $n = 4$ ). \*\*\* $P < 0.001$  versus anti-IgG. (B) Western blot analysis of *Mettl3* knockdown efficiency. *GAPDH* was used as the loading control. (C) Transcript levels of *linc1281* and *Mettl3* in shControl and shMettl3 mESCs. Error bars show  $\pm$  SEM ( $n = 3$ ). \*\* $P < 0.01$  versus shControl. (D) Changes in m<sup>6</sup>A-modified *linc1281* levels upon *Mettl3* depletion. The percentage of the input is shown. Error bars show  $\pm$  SEM ( $n = 3$ ). \*\* $P < 0.01$  versus shControl. (E) Schematic representation of the position of m<sup>6</sup>A motifs within *linc1281*. (F) Levels of *linc1281* transcripts in HEK293FT cells transfected with *linc1281*-overexpressing plasmids or mutants. ND, not detected. *linc1281*, Fuv-*linc1281*; A-G mutant, mutant with A-G transition mutations; A-T mutant, mutant with A-T transversion mutations; A-Del mutant, mutant with adenine residues deletion; NC mutant, negative control mutant with A<sup>916, 1024 and 1054</sup>-G transition mutations; A<sup>916</sup>-G mutant, mutant with A<sup>916</sup>-G transition mutation. Error bars show  $\pm$  SEM ( $n = 3$ ). \*\* $P < 0.01$  versus *linc1281*. (G) Changes in m<sup>6</sup>A-modified *linc1281* levels between *linc1281* and mutants in HEK293FT cells. The human transcript *GAPDH* was used as negative control. The percentage of the input is shown. Error bars show  $\pm$  SEM ( $n = 3$ ). \*\*\* $P < 0.001$ , \* $P < 0.05$  versus *linc1281*. (H) Levels of *linc1281* in shControl and shlinc1281 mESCs in the presence of the indicated overexpression constructs. shCtrl, shControl; sh1, shlinc1281-1; sh2, shlinc1281-2; FlucC, Fuv-luciferase Control. (I-K) Expression of cardiomyocyte markers on day 10 (I), percentage of beating EBs (J) and representative images of bodies stained for cTnT and Ho.33342 (K) on day 12 during EB formation. Scale bar represents 100  $\mu$ m. Error bars show  $\pm$  SEM ( $n = 3$ ). The asterisk (\*) denotes a significant difference from 'shCtrl+FlucC', and the hash mark (#) denotes a significant difference from 'sh1+FlucC' or 'sh2+FlucC'. ### $P < 0.001$ , \*\* $P < 0.01$ , \* $P < 0.05$ . (L-N) Percentage of Sox1<sup>+</sup> cells (L), expression of neural markers (M) and representative images of cells stained for Sox1-GFP, N-cad and Ho.33342 (N) on day 5 of neural differentiation. Scale bar represents 100  $\mu$ m. Error bars show  $\pm$  SEM ( $n \geq 3$ ). The asterisk (\*) denotes a significant difference from 'shCtrl+FlucC', and the hash mark (#) denotes a significant difference from 'sh1+FlucC' or 'sh2+FlucC'. \*\*\* $P < 0.001$ , \*\* $P < 0.01$ , \* $P < 0.05$ .

harbor no homologous RNA, with equal amounts of wild-type *linc1281*-overexpressing plasmids or mutants. The mutations were not related to transcript levels, as *linc1281* showed no significant difference between the wild-type- and mutant-transfected HEK293FT cells (Figure 2F). As expected, the m<sup>6</sup>A level on *linc1281* was decreased drastically upon destruction of the m<sup>6</sup>A motifs, confirming that the three identified motifs located in the last exon are predominantly responsible for the m<sup>6</sup>A modification of *linc1281* (Figure 2G). Accordingly, m<sup>6</sup>A-seq analysis of mESCs in a previous study (26) showed that the m<sup>6</sup>A peak within *linc1281* overlapped with the three m<sup>6</sup>A motifs (Supplementary Figure S4). In addition, the m<sup>6</sup>A enrichment of wild-type *linc1281* verified that the functions of the m<sup>6</sup>A methylase complex are evolutionarily conserved in humans and mice.

To assess the relationship between m<sup>6</sup>A and the regulatory functions of *linc1281* in mESCs, we stably overexpressed *linc1281*, the m<sup>6</sup>A-deficient A-G mutant or the m<sup>6</sup>A-decorated NC mutant using lentiviral vectors in *linc1281*-knockdown (sh1281) mESCs and performed *in vitro* differentiation assays. qRT-PCR analysis showed that the expression of *linc1281* was restored in sh1281 mESCs following the introduction of either wild-type *linc1281* or mutants, which were designated as follows: ‘sh1281+*linc1281* (sh1+*linc1281* and sh2+*linc1281*)’; ‘sh1281+A-G mutant (sh1+A-G mutant and sh2+A-G mutant)’; and sh1281+NC mutant (sh1+NC mutant and sh2+NC mutant), respectively (Figure 2H). As expected, the ‘sh1281+*linc1281*’ cell lines displayed a significantly increased EB differentiation efficiency, as evidenced by increases in cardiomyocyte markers (Figure 2I), the percentage of beating EBs (Figure 2J) and the number of cTnT-positive cells (Figure 2K), compared with ‘sh1281+FlucC (sh1+FlucC and sh2+FlucC)’ mESCs. However, ‘sh1281+A-G mutant’ cells exhibited limited differentiation. Similar to the observations made under EB differentiation, upon directed differentiation to the neural lineage, the ‘sh1281+*linc1281*’, but not the ‘sh1281+A-G mutant’ cells, showed substantially improved neural generation (Figure 2L-N). Notably, there was no significant difference in *linc1281* expression levels between ‘sh1281+*linc1281*’ and ‘sh1281+A-G mutant’ cells (Figure 2H); thus, we ruled out the possibility that the marked difference between the abilities of the two cell types was correlated with *linc1281* transcript abundance. These findings, coupled with the observation that A-G mutation resulted in much lower m<sup>6</sup>A levels than in wild-type *linc1281*, indicated that sufficient m<sup>6</sup>A modification is necessary for *linc1281* to regulate mESC differentiation. Expectedly, the NC mutant, marked with the m<sup>6</sup>A modification restored the differentiation capacity of *linc1281*-deficient mESCs (Figure 2I-N), which further confirmed the direct involvement of the m<sup>6</sup>A modification and functions of *linc1281* in mESCs. Consistently, *linc1281* but not the A-G mutant could restore the differentiation capacity of *linc1281* KO cells (Supplementary Figure S5).

### ***Linc1281* functions as an endogenous let-7 family sponge in mESCs**

In further exploring the underlying molecular mechanism by which m<sup>6</sup>A-modified *linc1281* controls the mESC differentiation capacity, we noted that *linc1281* was enriched in the cytoplasm of mESCs (Figure 1B-C). Previous studies have led to the conclusion that transcript abundance in the cytoplasm indicates that lincRNAs serve as ceRNAs, as posttranscriptional regulation of gene expression by miRNAs occurs preferentially in this subcellular compartment (42,43). Therefore, we predicted and screened the candidate targets of *linc1281*, especially miRNAs regulating mESC pluripotency, using the bioinformatics tool miRanda (44). We focused on the let-7/Lin28 axis because the entire let-7 family was predicted to exhibit strong direct binding with *linc1281*, and the important role of the let-7/Lin28 pathway in regulating stem cell pluripotency has been well-characterized (45,46) (Figure 3A). Since the miRNA/target ratio is functionally significant, we detected the absolute levels of *linc1281* and let-7 miRNAs in mESCs and observed that *linc1281* and let-7 miRNAs were expressed at the same order of magnitude (Supplementary Figure S6), which supported our hypothesis for the ceRNA model based on previous reports (47–49). To probe the connection between the two populations, we constructed luciferase reporters containing full-length *linc1281* in the 3' UTR of the luciferase gene. The reporters were cotransfected into NIH/3T3 cells with miRNA mimics. The let-7 mimics significantly reduced the luciferase activities of the *linc1281* reporters compared with the control mimics (Figure 3B). Furthermore, to test the specificity of let-7 binding to predicted target sites, we constructed mutant luciferase reporters containing a 7-bp antisense mismatch within the target site of let-7 and found that the wild-type reporters showed significantly decreased luciferase activity when cotransfected with let-7 mimics, whereas the mutant reporters were refractory to let-7-driven reporter inhibition (Figure 3C). To further confirm the direct binding of let-7 to *linc1281* transcripts, we also performed an RNA immunoprecipitation (RIP) assay with the MS2-binding protein (MS2bp), which specifically binds RNA containing the MS2-binding sequence (MS2bs) (36). The vector (MS2bs-*linc1281*) expressing *linc1281* combined with MS2bs elements was cotransfected into HEK293FT cells with the vector encoding MS2bp-YFP and let-7 mimics. The vector (MS2bs-*Renilla*) expressing *Renilla* luciferase RNA was used as a negative control. The transcript-specific binding RNA-protein complexes were immunoprecipitated with a YFP antibody and then analyzed via qRT-PCR. Immunoglobulin G (IgG) was used as a negative control. We found that let-7 miRNAs were enriched in MS2bs-*linc1281*-binding RNAs compared with the negative control (Figure 3D).

Next, to further explore the interaction of *linc1281* and let-7 miRNAs in a more physiological context, we transfected mESCs with MS2bs-*linc1281* or MS2bs-*Renilla* combined with MS2bp-YFP and performed RIP assays. As expected, let-7 miRNAs were expressed in mESCs and showed significant enrichment in MS2bs-*linc1281*-binding RNAs compared with the MS2bs-*Renilla* control (Figure 3E). Previous studies have demonstrated that as a ceRNA, lincR-

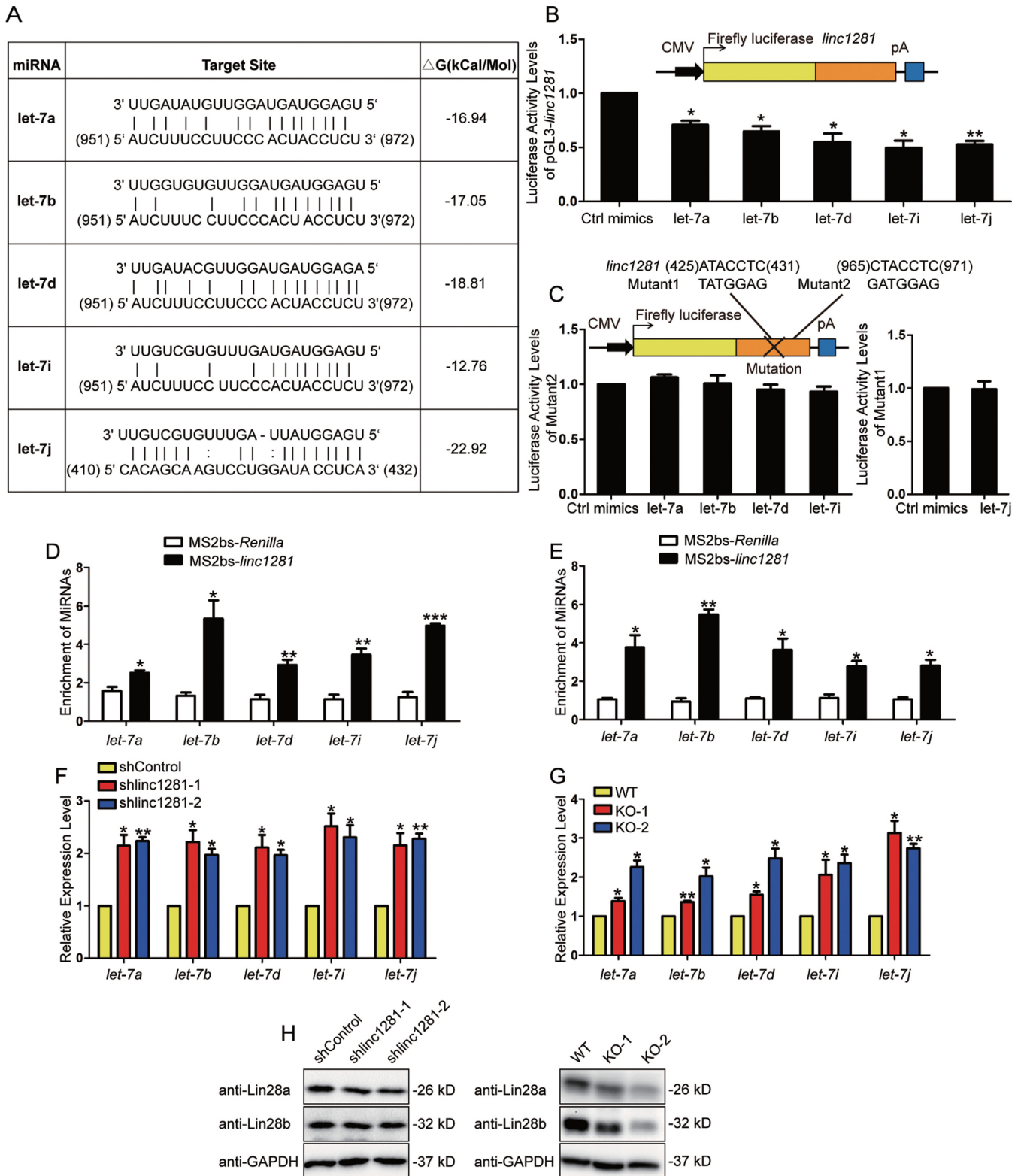


**Figure 3.** *Linc1281* functions as a ceRNA of the let-7 family in mESCs. (A) Summary of let-7 family target sites in *linc1281*. (B and C) Relative luciferase activities of reporters containing *linc1281* (pGL3-*linc1281*, B) or mutants (C) in NIH/3T3 cells 48 hr after cotransfection with the indicated miRNAs or the scramble negative control (Ctrl mimics). Firefly luciferase activity was normalized to control Renilla luciferase activity. pA, polyadenylation signal. Error bars show  $\pm$  SEM ( $n = 3$ ).  $**P < 0.01$ ,  $*P < 0.05$  versus Ctrl mimics. (D and E) Enrichment of immunoprecipitated miRNAs in HEK293FT cells (D) or mESCs (E). MS2bs-*Renilla* luciferase RNA was used as a negative control. The fold enrichment relative to the IgG control is shown. Error bars show  $\pm$  SEM ( $n = 3$ ).  $***P < 0.001$ ,  $**P < 0.01$ ,  $*P < 0.05$  versus MS2bs-*Renilla*. (F and G) Expression levels of mature let-7 miRNAs in mESCs upon *linc1281* knockdown (F) or knockout (G). SnoRNA U6 was used as an internal control for normalization. Error bars show  $\pm$  SEM ( $n = 3$ ).  $**P < 0.01$ ,  $*P < 0.05$  versus shControl or WT. (H) Representative western blot analysis of Lin28a and Lin28b in mESCs upon *linc1281* depletion. GAPDH was used as the loading control.

NAs can influence miRNA expression (35,36). Thus, we examined miRNA levels and found that mature let-7 miRNAs were substantially increased in *linc1281*-knockdown and *linc1281*-knockout mESCs (Figure 3F and G), suggesting that let-7 miRNAs are inversely associated with *linc1281* levels. In addition, following an increase in let-7 family abundance, the Lin28 RNA-binding proteins, which are the critical targets of let-7 miRNAs, displayed significantly reduced protein levels (Figure 3H), which confirmed that *linc1281* indeed regulates the let-7/Lin28 axis.

Collectively, these findings indicated that *linc1281* serves as a ceRNA through direct binding with let-7 miRNAs in mESCs.

### The m<sup>6</sup>A modification is necessary for the *linc1281*-mediated ceRNA model

To determine the relationship between the m<sup>6</sup>A modification of *linc1281* and *linc1281*-mediated RNA-miRNA interactions, we first examined the expression levels of let-7 miRNAs in ‘sh1281+*linc1281*’, ‘sh1281+A-G mutant’ and ‘sh1281+NC mutant’ mESCs. We found that ‘sh1281+*linc1281*’ and ‘sh1281+NC mutant’ cells showed decreased let-7 miRNA levels compared with ‘sh1281+Fluc’ cells (Figure 4A). However, the ‘sh1281+A-G mutant’ population still displayed high miRNA levels, despite the fact that we observed no difference in *linc1281* transcript levels between these cell types. Coupled with the observation that the A-G mutant contained an insufficient level of the m<sup>6</sup>A modification, we hypothesized that m<sup>6</sup>A on *linc1281* may be involved in the direct RNA-RNA interaction. Thus, we established a Mettl3 knockdown NIH/3T3 cell line using shRNA, which exhibited at least 80% reduction of the endogenous Mettl3 protein (Figure 4B). Cells infected with lentivirus containing scrambled shRNA were used as control cells. Then, we performed luciferase reporter assays in shControl and shMettl3 cells after transfection with the *linc1281* reporter and miRNA mimics. The significant decrease in luciferase activity observed in control cells suggested direct binding and regulation of *linc1281* by miRNAs, which was consistent with the previous results (Figure 4C). However, the effect of let-7 miRNAs on the *linc1281* reporter was abolished upon Mettl3 knockdown, as reporter activity showed no change upon cotransfection with let-7 miRNAs in shMettl3 cells (Figure 4D). These results revealed that the m<sup>6</sup>A methyltransferase Mettl3 is critical for the binding of mature let-7 miRNA to *linc1281*. We overexpressed wild-type Mettl3 (WT) or a catalytically dead mutant of Mettl3 (Mut; residues 395–399: DPPW-APPA) (14,50) in shMettl3 mESCs (Figure 4E) and detected the m<sup>6</sup>A levels of *linc1281* in these cell lines. Restoration of the m<sup>6</sup>A modification of *linc1281* by wild-type Mettl3, but not the Mettl3 mutant, further confirmed that the m<sup>6</sup>A modification of *linc1281* is dependent on the enzymatic activity of Mettl3 (Figure 4F). Then, we introduced Mettl3 and the mutant into Mettl3 knockdown NIH/3T3 cells (Figure 4G) and performed luciferase reporter assays. Despite the equal expression levels of Mettl3 and the mutant in shMettl3 cells, the abolished effect of let-7 miRNAs on the *linc1281* reporter in shMettl3 cells was restored by Mettl3,

but not by the catalytically dead mutant (Figure 4H-I), which further suggested that the Mettl3-dependent m<sup>6</sup>A modification of *linc1281* is necessary for *linc1281*-miRNA interactions.

To rule out the possibility that this result was caused by a Mettl3 deficiency-mediated decrease in the widespread m<sup>6</sup>A modification in shMettl3 cells, we constructed luciferase reporters containing an m<sup>6</sup>A-deficient mutant in the 3' UTR of the luciferase gene. We then transfected wild-type NIH/3T3 cells with let-7 miRNA mimics combined with wild-type *linc1281* or m<sup>6</sup>A mutant reporters and measured the resultant luciferase activities. As expected, let-7 miRNAs decreased luciferase activities in the presence of wild-type *linc1281* (Figure 4J), while they showed no effect on the m<sup>6</sup>A-deficient mutant reporters (Figure 4K and Supplementary Figure S7A-B). Expectedly, let-7 miRNAs showed a significant effect on the negative control mutant reporters (Supplementary Figure S7C and D). Then, we performed luciferase reporter assays in shControl and shMettl3 cells after transfection with miRNA mimics combined with the NC or A-G mutant reporters and observed that A-G mutation abolished the effect of miRNAs on NC reporter in the presence of Mettl3 (Supplementary Figure S7E), while the luciferase activities showed no difference between NC and A-G mutant reporters in shMettl3 cells (Supplementary Figure S7F). Collectively, these results provided strong evidence that m<sup>6</sup>A enrichment of *linc1281* is required for the *linc1281*-mediated ceRNA model.

### The let7/Lin28 pathway fully restores the differentiation capacity in m<sup>6</sup>A-*linc1281*-deficient mESCs

Next, we asked whether the ceRNA model is responsible for the *linc1281*-mediated regulation of mESC differentiation. We constructed let-7 miRNA sponges, which served as decoy targets for miRNAs, as described in a previous study (51), and then established let-7 family sponge-expressing mESCs, in which *linc1281* was also knocked down. Examination of miRNA levels via qRT-PCR showed that the sponges effectively inhibited let-7 family expression, which was increased by *linc1281* deficiency (Supplementary Figure S8A). Through phenotypic analysis during mESC differentiation, we found that concomitant expression of the let-7 sponge was sufficient to rescue the impaired mESC differentiation capacity after *linc1281* knockdown, as shown by upregulation of cardiomyocyte markers (Figure 5A), an increased percentage of beating EBs (Figure 5B) and enhanced cTnT-positive cell numbers (Figure 5C) in EB assays, together with increases in Sox1<sup>+</sup> cells (Figure 5D), levels of neural genes (Figure 5E) and Sox1-GFP/N-cad-positive cells (Figure 5F) in neural differentiation. These results confirmed that let-7 miRNAs were indeed functional targets of *linc1281*. Moreover, since Lin28 proteins, which are the direct targets of the let-7 family and critical pluripotency factors in mESCs, showed decreased levels upon *linc1281* knockdown (Figure 3H), we also tested whether Lin28 contributed to the underlying mechanism of the *linc1281*-let-7 model. For this purpose, we overexpressed Lin28a or Lin28b in *linc1281* knockdown mESCs (Supplementary Figure S8B) and examined the differentiation of these cell lines, revealing that overexpression of Lin28 re-

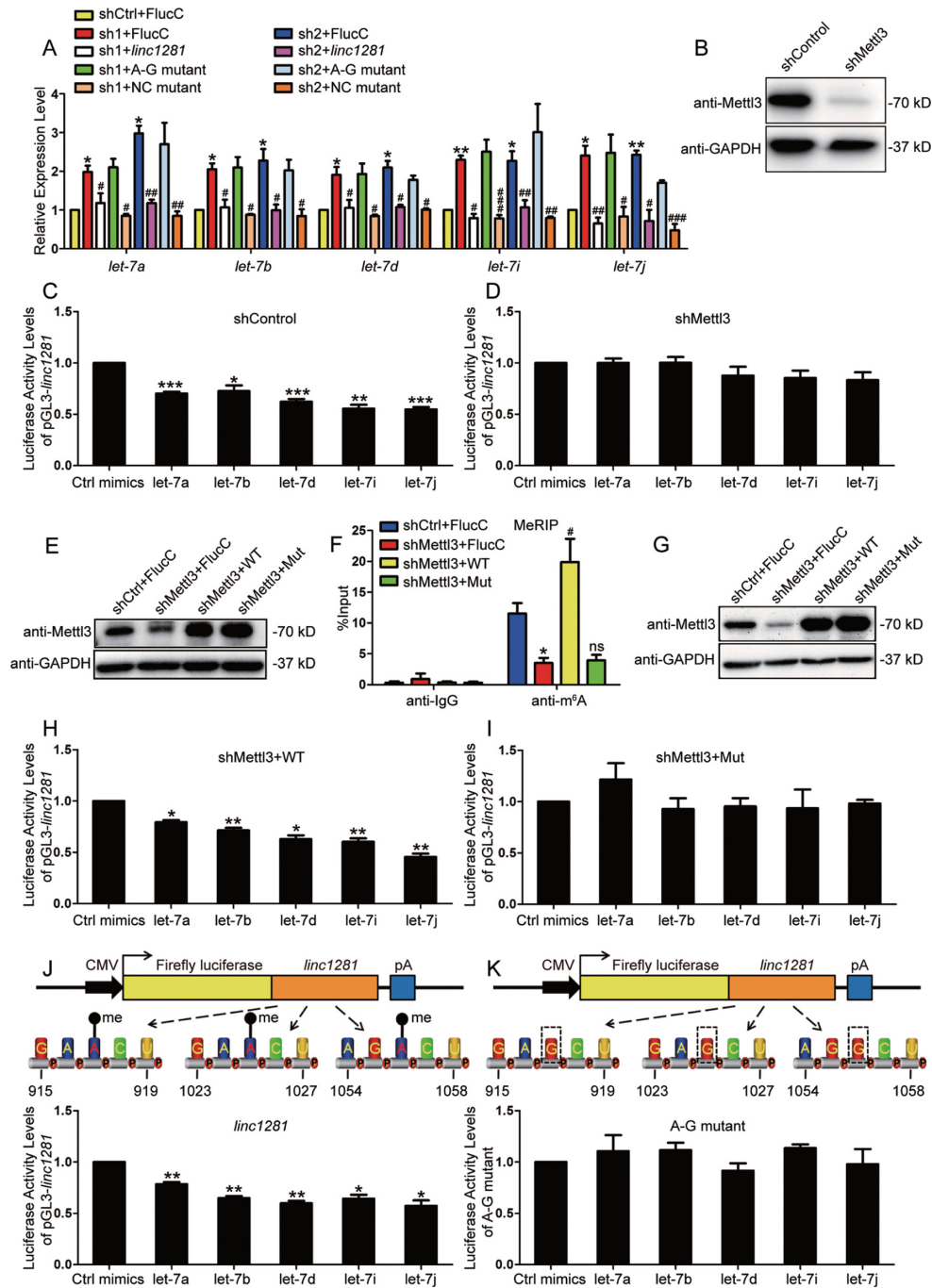


**Figure 4.** The  $m^6A$  mark is critical for the functional role of *linc1281* as a natural decoy. (A) Expression levels of mature let-7 miRNAs in shControl and sh*linc1281* mESCs in the presence of the indicated overexpression constructs. SnoRNA U6 was used as an internal control for normalization. Error bars show  $\pm$  SEM ( $n = 3$ ). The asterisk (\*) denotes a significant difference from 'shCtrl+FlucC', and the hash mark (#) denotes a significant difference from 'sh1+FlucC' or 'sh2+FlucC'. ### $P < 0.001$ , \*\* $P < 0.01$ , \* $P < 0.05$ . (B) Western blot analysis of Mettl3 knockdown efficiency in shMettl3 NIH/3T3 cells. GAPDH was used as the loading control. (C and D) The relative luciferase activities of reporters containing *linc1281* in shControl (C) and shMettl3 (D) NIH/3T3 cells 48 hr after cotransfection with the indicated miRNAs or Ctrl mimics. Firefly luciferase activity was normalized to control Renilla luciferase activity. Error bars show  $\pm$  SEM ( $n = 4$ ). \*\*\* $P < 0.001$ , \*\* $P < 0.01$ , \* $P < 0.05$  versus Ctrl mimics. (E) Western blot for Mettl3 in shControl and shMettl3 mESCs in the presence of the indicated overexpression constructs. WT, wild-type Mettl3; Mut, catalytically inactive mutant of Mettl3. GAPDH was used as the loading control. (F) Wild-type Mettl3, but not the mutant, restored the  $m^6A$  modification of *linc1281* in Mettl3 knockdown mESCs in MeRIP assays. The percentage of the input is shown. Error bars show  $\pm$  SEM ( $n = 4$ ). \* $P < 0.05$  versus 'shCtrl+FlucC'; # $P < 0.05$  versus 'shMettl3+FlucC'; ns, non-significant against 'shMettl3+FlucC'. (G) Western blotting of Mettl3 in the indicated NIH/3T3 cells. GAPDH was used as the loading control. (H-I) pGL3-*linc1281* reporter assays in 'shMet3+WT' (H) and 'shMettl3+Mut' (I) NIH/3T3 cells 48 h after cotransfection with the indicated miRNAs or Ctrl mimics. Firefly luciferase activity was normalized to control Renilla luciferase activity. Error bars show  $\pm$  SEM ( $n = 3$ ). \*\* $P < 0.01$ , \* $P < 0.05$  versus Ctrl mimics. (J-K) Relative luciferase levels of pGL3-*linc1281* and A-G mutant reporters 48 hr after cotransfection with the indicated miRNAs or Ctrl mimics. Firefly luciferase activity was normalized to control Renilla luciferase activity. Error bars show  $\pm$  SEM ( $n = 3$ ). \*\* $P < 0.01$ , \* $P < 0.05$  versus Ctrl mimics.

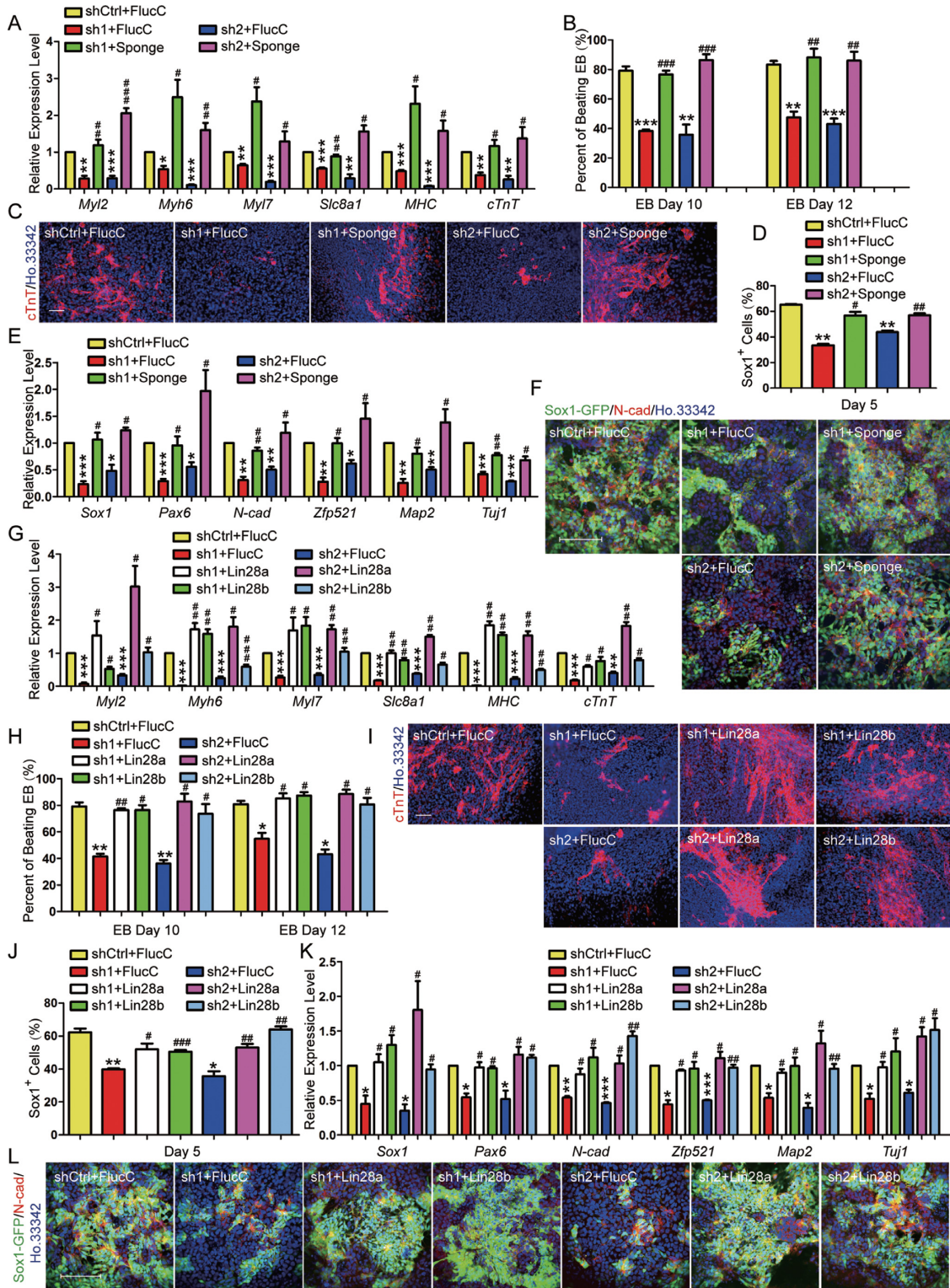


**Figure 5.** The let-7/Lin28 pathway restores the impaired capacity of mESCs in the absence of m<sup>6</sup>A-*linc1281*. (A) qRT-PCR analysis of cardiomyocyte markers on day 10 of EB differentiation in shControl and shlinc1281 mESCs in the presence of FlucC or the let-7 miRNA sponge. Sponge, the construct expresses a sponge RNA that contains three tandemly repeated complementary binding sites to each of the 5 miRNAs. (B) Percentage of beating EBs. (C) Representative images of bodies stained for cTnT and Ho.33342 on day 12 of EB formation. (D–F) FACS isolation of Sox1<sup>+</sup> cells (D), qRT-PCR analysis of neural markers (E) and representative images of cells stained for Sox1-GFP, N-cad and Ho.33342 on day 5 of neural differentiation (F). (G–I) The spontaneous differentiation capacity of shControl and shlinc1281 mESCs overexpressing FlucC, Lin28a or Lin28b, based on EB formation. (J–L) Examination of the neural lineage differentiation capacity of the indicated mESC lines. Scale bar represents 100 μm. Error bars show ± SEM (*n* ≥ 3). The asterisk (\*) denotes a significant difference from ‘shCtrl+FlucC’, and the hash mark (#) denotes a significant difference from ‘sh1+FlucC’ or ‘sh2+FlucC’. \*\*\*, ### *P* < 0.001, \*\*, ## *P* < 0.01, \*, # *P* < 0.05.

stored the phenotype caused by *linc1281* deficiency (Figure 5G-L).

Collectively, our results showed that *linc1281* is required for proper differentiation of mESCs and that this critical function relies upon sufficient enrichment of the m<sup>6</sup>A modification on *linc1281* via an m<sup>6</sup>A-dependent model in which m<sup>6</sup>A-modified *linc1281* attenuates let-7 miRNAs and then regulates the let-7/Lin28 pathway (Supplementary Figure S8C).

## DISCUSSION

The requirement of lincRNAs for the maintenance of mESC pluripotency has been demonstrated through systematic loss-of-function experiments (6), but relatively little is known about the functional role of individual lincRNAs in mESCs, and it is unclear how lincRNAs epigenetically modulate mESC self-renewal and cell-fate decisions. The identification of specific lincRNAs has shown the importance of lincRNAs in developmental biology and promotes our understanding of the posttranscriptional regulatory network maintaining mESC identities. In this study, we characterized the role of *linc1281* in controlling mESC pluripotency. We found that *linc1281* serves as a mESC-specific RNA and is required for proper mESC differentiation.

The let-7/Lin28 pathway has been identified as an essential regulator of early embryonic development and mESC pluripotency (46,52). Let-7 miRNAs repress Lin28 mRNA translation, which in turn inhibits miRNA biogenesis (53,54). Transcription factors and miRNAs regulate the expression level and function of let-7 by directly targeting Lin28 (46,52). While most studies have focused on the regulation of miRNA transcription and processing, here, we showed that mature let-7 levels were modulated by *linc1281*, which contributes to the complexity and stability of the regulatory network involved in the let-7/Lin28 pathway. In addition, precise control of mature let-7 miRNAs enables a rapid response to differentiation cues compared with primary regulation at the level of the transcription and processing of pri-miRNAs or pre-miRNAs. Thus, we propose that the lincRNA-mediated ceRNA model is a flexible and effective modulator in mESCs. Coincidentally, *linc1281* was very recently identified as a ‘regulator of naïve ESC transition’ by indirectly targeting Lin28a, although the underlying mechanism remains unclear (55). In our model, *linc1281* functions as a posttranscriptional modulator by directly interacting with let-7 miRNAs and subsequently regulates the miRNA target Lin28. We hypothesize that *linc1281*-miRNA interaction might also contribute to naïve ESC transition and that *linc1281* regulates the pluripotency and differentiation potential of ESCs by acting as a multi-layered control machinery.

The m<sup>6</sup>A modification is widespread throughout the transcriptome, accounting for 0.1–0.4% of total adenosine residues in native cellular RNAs. As one of the most common RNA modifications, m<sup>6</sup>A is found on almost all types of RNAs and has been implicated in a variety of cellular processes, including mRNA metabolism (9–13,15,16), miRNA biogenesis (14) and m<sup>6</sup>A-derived circular RNA translation (56). However, the functions of m<sup>6</sup>A

in lincRNAs remain undefined. Here, we first proposed an m<sup>6</sup>A-dependent model of lincRNA/miRNA interaction in mESCs, in which m<sup>6</sup>A modification of *linc1281* is required for the direct binding of let-7 to *linc1281*. The lincRNA-mediated ceRNA pathway plays a key role in regulating gene activities and has been documented in several studies. Since the crosstalk between lincRNAs and miRNAs is always mediated via a simple sequence pairing mechanism, whether modulators regulate this interaction has not yet been explored. Our study identified m<sup>6</sup>A as a positive mediator in the ceRNA model, which is supported by the observation that the m<sup>6</sup>A-deficient A-G mutant abolished the interaction between *linc1281* and let-7 miRNAs. Furthermore, in the absence of Mettl3, *linc1281* exhibited decreased m<sup>6</sup>A levels and lacked the ability to bind let-7 miRNAs, suggesting that Mettl3 is predominantly responsible for m<sup>6</sup>A lincRNA methylation and the m<sup>6</sup>A-mediated ceRNA model. These observations were supported by the fact that wild-type Mettl3, but not an enzymatically inactive mutant, restored the m<sup>6</sup>A modification of *linc1281* and the RNA-RNA interaction. The identification of individual m<sup>6</sup>A-marked lincRNAs has additional value in clarifying the functions of Mettl3-dependent RNA modification in the field of RNA epigenetics. Intriguingly, previous research revealed that 67% of mRNA 3'UTRs that contain m<sup>6</sup>A peaks also contain miRNA binding sites, and the overall distribution of these two groups shows an anti-correlated relationship (57,58), suggesting a possible mechanism by which m<sup>6</sup>A might cooperate or compete with miRNAs to regulate target mRNAs. Here, we propose a model in which lincRNAs contain both m<sup>6</sup>A peaks and miRNA binding sites, where m<sup>6</sup>A cooperates with the miRNA pathway to operate the lincRNA-mediated regulation of pluripotency targets and control the differentiation of mESCs, adding a layer of complexity to our knowledge of the molecular events modulating RNA-miRNA interactions and providing insights into the lincRNA modification-mediated regulatory network in mESCs. Since m<sup>6</sup>A could alter the local structure of RNA (59) and thus, enhance the RNA bindings of hnRNPs, we identified *linc1281*-interacting proteins by performing biotinylated *linc1281* RNA pull down and LC/MS experiments (Supplementary Table S1) and further explored whether *linc1281* binding hnRNPs affect the m<sup>6</sup>A-dependent RNA-miRNA interactions. However, let-7 miRNAs still significantly decreased the luciferase activities of *linc1281* reporters in the absence of defined hnRNPs (Supplementary Figure S9). To detect the possibly undiscovered RBPs in the large number of proteins bound to *linc1281* in the future is useful for the elucidation of the detailed mechanisms of the m<sup>6</sup>A-mediated *linc1281*-miRNA interaction in mESC behaviors.

m<sup>6</sup>A has emerged as a critical fate determinant in mESCs, and genetic inactivation or depletion of the m<sup>6</sup>A methylase Mettl3, and hence m<sup>6</sup>A, disrupts normal lineage priming and differentiation (10,26). While all studies performed to date suggest that the m<sup>6</sup>A-decorated mRNAs of mESC pluripotency factors, such as Sox2 and Nanog, play an essential role in the m<sup>6</sup>A-mediated control of mESC features, the function of m<sup>6</sup>A in mESC-specific lincRNAs, which are also integral components of the mESC regulatory network, is unclear. In the present work, we showed that m<sup>6</sup>A

is enriched on *linc1281*, and this modification is responsible for the *linc1281*-mediated control of mESC identities, as impairment of the mESC differentiation capacity upon *linc1281* loss can be rescued by wild-type *linc1281*, but not by the m<sup>6</sup>A modification-deficient A-G mutant. The necessity of m<sup>6</sup>A for the *linc1281*-mediated maintenance of mESC differentiation further stresses the requirement of the m<sup>6</sup>A modification for mESC pluripotency. Several reports have proposed that the decreased stability of methylated core mESC transcripts contributes to Mettl3-deficient mESC phenotypes (10,26,60). Therefore, in undifferentiated mESCs, pluripotency-related transcripts tend to exhibit relatively low m<sup>6</sup>A levels. This hypothesis was supported by the identification of ZFP217, which functions to sequester Mettl3 and prevents the methylation of core mESC transcripts (25). Nevertheless, it remains unclear whether m<sup>6</sup>A plays a positive role in modulating the pluripotent regulatory circuitry, as the methyltransferase Mettl3 shows high levels and activity in undifferentiated mESCs (25,26,61). Conceptually, we propose that m<sup>6</sup>A in *linc1281* is required for the role of *linc1281* in mESC pluripotency regulatory networks and is positively involved in the *linc1281*-mediated maintenance of the mESC differentiation capacity. This model suggests that the m<sup>6</sup>A modification of lincRNA is an important component of the complex regulatory network driven by RNA methylation and reveals how m<sup>6</sup>A regulates the physiological functions of lincRNAs. Since the study of the biological role of RNA methylation is still in its infancy, additional discoveries of regulatory patterns mediated by m<sup>6</sup>A will help elucidate the overall function of RNA methylation.

In summary, we have demonstrated that m<sup>6</sup>A-*linc1281* is critical for proper differentiation of mESCs and identified a novel role of m<sup>6</sup>A as a necessary flexibility factor in maintaining mESC identities.

## SUPPLEMENTARY DATA

Supplementary Data are available at NAR Online.

## ACKNOWLEDGEMENTS

J.K. conceived and designed the research; D.Y. performed experiments, designed experiments, analyzed data and wrote the paper; J.Q. and Y.L. performed experiments; G.L., X.G. and D.Y. designed experiments; G.W. edited the manuscript. S.Z., J.X. and W.C. revised the article. Y.L. and X.W. reviewed the study.

## FUNDING

Ministry of Science and Technology [2016YFA0101300]; National Natural Science Foundation of China [81530042, 31721003, 31571529, 31571519, 31471250, 31701110, 31571390, 31771506, 81600675, 31671533]; Ministry of Education Grants IRT.15R51, Science and Technology Commission of Shanghai Municipality [15JC1403201]; Fundamental Research Funds for the Central Universities [1500219106, 20002310002, 1515219039, 1515219040]. Funding for open access charge: Ministry of Science and Technology [2016YFA0101300]; National Natural Science Foundation of China [81530042, 31721003,

31571529, 31571519, 31471250, 31701110, 31571390, 31771506, 81600675, 31671533]; Ministry of Education Grants IRT.15R51, Science and Technology Commission of Shanghai Municipality [15JC1403201]; Fundamental Research Funds for the Central Universities [1500219106, 20002310002, 1515219039, 1515219040].

*Conflict of interest statement.* None declared.

## REFERENCES

- Young, R.A. (2011) Control of the embryonic stem cell state. *Cell*, **144**, 940–954.
- Chen, X., Xu, H., Yuan, P., Fang, F., Huss, M., Vega, V.B., Wong, E., Orlov, Y.L., Zhang, W., Jiang, J. *et al.* (2008) Integration of external signaling pathways with the core transcriptional network in embryonic stem cells. *Cell*, **133**, 1106–1117.
- Wang, K.C. and Chang, H.Y. (2011) Molecular mechanisms of long noncoding RNAs. *Mol. Cell*, **43**, 904–914.
- Guttman, M., Garber, M., Levin, J.Z., Donaghey, J., Robinson, J., Adiconis, X., Fan, L., Koziol, M.J., Gnirke, A., Nussbaum, C. *et al.* (2010) Ab initio reconstruction of cell type-specific transcriptomes in mouse reveals the conserved multi-exonic structure of lincRNAs. *Nat. Biotechnol.*, **28**, 503–510.
- Guttman, M., Amit, I., Garber, M., French, C., Lin, M.F., Feldser, D., Huarte, M., Zuk, O., Carey, B.W., Cassady, J.P. *et al.* (2009) Chromatin signature reveals over a thousand highly conserved large non-coding RNAs in mammals. *Nature*, **458**, 223–227.
- Guttman, M., Donaghey, J., Carey, B.W., Garber, M., Grenier, J.K., Munson, G., Young, G., Lucas, A.B., Ach, R., Bruhn, L. *et al.* (2011) lincRNAs act in the circuitry controlling pluripotency and differentiation. *Nature*, **477**, 295–300.
- He, C. (2010) Grand challenge commentary: RNA epigenetics? *Nat. Chem. Biol.*, **6**, 863–865.
- Meyer, K.D. and Jaffrey, S.R. (2014) The dynamic epitranscriptome: N<sup>6</sup>-methyladenosine and gene expression control. *Nat. Rev. Mol. Cell Biol.*, **15**, 313–326.
- Wang, X., Lu, Z., Gomez, A., Hon, G.C., Yue, Y., Han, D., Fu, Y., Parisien, M., Dai, Q., Jia, G. *et al.* (2014) N<sup>6</sup>-methyladenosine-dependent regulation of messenger RNA stability. *Nature*, **505**, 117–120.
- Geula, S., Moshitch-Moshkovitz, S., Dominissini, D., Mansour, A.A., Kol, N., Salmon-Divon, M., Hershkovitz, V., Peer, E., Mor, N., Manor, Y.S. *et al.* (2015) Stem cells. m<sup>6</sup>A mRNA methylation facilitates resolution of naive pluripotency toward differentiation. *Science*, **347**, 1002–1006.
- Zhao, X., Yang, Y., Sun, B.F., Shi, Y., Yang, X., Xiao, W., Hao, Y.J., Ping, X.L., Chen, Y.S., Wang, W.J. *et al.* (2014) FTO-dependent demethylation of N<sup>6</sup>-methyladenosine regulates mRNA splicing and is required for adipogenesis. *Cell Res.*, **24**, 1403–1419.
- Lence, T., Akhtar, J., Bayer, M., Schmid, K., Spindler, L., Ho, C.H., Kreim, N., Andrade-Navarro, M.A., Poeck, B., Helm, M. *et al.* (2016) m<sup>6</sup>A modulates neuronal functions and sex determination in *Drosophila*. *Nature*, **540**, 242–247.
- Meyer, K.D., Patil, D.P., Zhou, J., Zinoviev, A., Skabkin, M.A., Elemento, O., Pestova, T.V., Qian, S.B. and Jaffrey, S.R. (2015) 5' UTR m<sup>6</sup>A Promotes Cap-Independent Translation. *Cell*, **163**, 999–1010.
- Alarcon, C.R., Lee, H., Goodarzi, H., Halberg, N. and Tavazoie, S.F. (2015) N<sup>6</sup>-methyladenosine marks primary microRNAs for processing. *Nature*, **519**, 482–485.
- Zhang, C., Samanta, D., Lu, H., Bullen, J.W., Zhang, H., Chen, I., He, X. and Semenza, G.L. (2016) Hypoxia induces the breast cancer stem cell phenotype by HIF-dependent and ALKBH5-mediated m<sup>6</sup>A-demethylation of NANOG mRNA. *Proc. Natl. Acad. Sci. U.S.A.*, **113**, E2047–E2056.
- Hausmann, I.U., Bodi, Z., Sanchez-Moran, E., Mongan, N.P., Archer, N., Fray, R.G. and Soller, M. (2016) m<sup>6</sup>A potentiates Sxl alternative pre-mRNA splicing for robust *Drosophila* sex determination. *Nature*, **540**, 301–304.
- Zhang, S., Zhao, B.S., Zhou, A., Lin, K., Zheng, S., Lu, Z., Chen, Y., Sulman, E.P., Xie, K., Bogler, O. *et al.* (2017) m<sup>6</sup>A demethylase ALKBH5 maintains tumorigenicity of glioblastoma stem-like cells by

- sustaining FOXM1 expression and cell proliferation program. *Cancer Cell*, **31**, 591–606.
18. Zhang, C., Chen, Y., Sun, B., Wang, L., Yang, Y., Ma, D., Lv, J., Heng, J., Ding, Y., Xue, Y. *et al.* (2017) m<sup>6</sup>A modulates haematopoietic stem and progenitor cell specification. *Nature*, **549**, 273–276.
  19. Cui, Q., Shi, H., Ye, P., Li, L., Qu, Q., Sun, G., Sun, G., Lu, Z., Huang, Y., Yang, C.G. *et al.* (2017) m<sup>6</sup>A RNA Methylation Regulates the Self-Renewal and Tumorigenesis of Glioblastoma Stem Cells. *Cell Rep.*, **18**, 2622–2634.
  20. Xiang, Y., Laurent, B., Hsu, C.H., Nachtergaele, S., Lu, Z., Sheng, W., Xu, C., Chen, H., Ouyang, J., Wang, S. *et al.* (2017) RNA m<sup>6</sup>A methylation regulates the ultraviolet-induced DNA damage response. *Nature*, **543**, 573–576.
  21. Zhao, B.S., Wang, X., Beadell, A.V., Lu, Z., Shi, H., Kuuspalu, A., Ho, R.K. and He, C. (2017) m<sup>6</sup>A-dependent maternal mRNA clearance facilitates zebrafish maternal-to-zygotic transition. *Nature*, **542**, 475–478.
  22. Lin, Z., Hsu, P.J., Xing, X., Fang, J., Lu, Z., Zou, Q., Zhang, K.J., Zhang, X., Zhou, Y., Zhang, T. *et al.* (2017) Mettl3-/Mettl14-mediated mRNA N<sup>6</sup>-methyladenosine modulates murine spermatogenesis. *Cell Res.*, **27**, 1216–1230.
  23. Yoon, K.J., Ringeling, F.R., Vissers, C., Jacob, F., Pokrass, M., Jimenez-Cyrus, D., Su, Y., Kim, N.S., Zhu, Y., Zheng, L. *et al.* (2017) Temporal control of mammalian cortical neurogenesis by m<sup>6</sup>A methylation. *Cell*, **171**, 877–889.
  24. Sibbritt, T., Patel, H.R. and Preiss, T. (2013) Mapping and significance of the mRNA methylome. *Wiley Interdiscip. Rev. RNA*, **4**, 397–422.
  25. Aguilo, F., Zhang, F., Sancho, A., Fidalgo, M., Di Cecilia, S., Vashisht, A., Lee, D.F., Chen, C.H., Rengasamy, M., Andino, B. *et al.* (2015) Coordination of m<sup>6</sup>A mRNA Methylation and Gene Transcription by ZFP217 Regulates Pluripotency and Reprogramming. *Cell Stem Cell*, **17**, 689–704.
  26. Batista, P.J., Molinie, B., Wang, J., Qu, K., Zhang, J., Li, L., Bouley, D.M., Lujan, E., Haddad, B., Daneshvar, K. *et al.* (2014) m<sup>6</sup>A RNA modification controls cell fate transition in mammalian embryonic stem cells. *Cell Stem Cell*, **15**, 707–719.
  27. Murchison, E.P., Partridge, J.F., Tam, O.H., Cheloufi, S. and Hannon, G.J. (2005) Characterization of Dicer-deficient murine embryonic stem cells. *Proc. Natl Acad. Sci. U.S.A.*, **102**, 12135–12140.
  28. Wang, Y., Medvid, R., Melton, C., Jaenisch, R. and Belloch, R. (2007) DGCR8 is essential for microRNA biogenesis and silencing of embryonic stem cell self-renewal. *Nat. Genet.*, **39**, 380–385.
  29. Kanellopoulou, C., Muljo, S.A., Kung, A.L., Ganesan, S., Drapkin, R., Jenuwein, T., Livingston, D.M. and Rajewsky, K. (2005) Dicer-deficient mouse embryonic stem cells are defective in differentiation and centromeric silencing. *Genes Dev.*, **19**, 489–501.
  30. Tay, Y.M., Tam, W.L., Ang, Y.S., Gaughwin, P.M., Yang, H., Wang, W., Liu, R., George, J., Ng, H.H., Perera, R.J. *et al.* (2008) MicroRNA-134 modulates the differentiation of mouse embryonic stem cells, where it causes post-transcriptional attenuation of Nanog and LRH1. *Stem Cells*, **26**, 17–29.
  31. Xu, N., Papagiannakopoulos, T., Pan, G., Thomson, J.A. and Kosik, K.S. (2009) MicroRNA-145 regulates OCT4, SOX2, and KLF4 and represses pluripotency in human embryonic stem cells. *Cell*, **137**, 647–658.
  32. Yang, D., Wang, G., Zhu, S., Liu, Q., Wei, T., Leng, Y., Duan, T. and Kang, J. (2014) MiR-495 suppresses mesoderm differentiation of mouse embryonic stem cells via the direct targeting of Dnm3a. *Stem Cell Res.*, **12**, 550–561.
  33. Melton, C., Judson, R.L. and Belloch, R. (2010) Opposing microRNA families regulate self-renewal in mouse embryonic stem cells. *Nature*, **463**, 621–626.
  34. Cesana, M., Cacchiarelli, D., Legnini, I., Santini, T., Sthandier, O., Chinappi, M., Tramontano, A. and Bozzoni, I. (2011) A long noncoding RNA controls muscle differentiation by functioning as a competing endogenous RNA. *Cell*, **147**, 358–369.
  35. Durruthy-Durruthy, J., Sebastiano, V., Wossidlo, M., Cepeda, D., Cui, J., Grow, E.J., Davila, J., Mall, M., Wong, W.H., Wysocka, J. *et al.* (2016) The primate-specific noncoding RNA HPAT5 regulates pluripotency during human preimplantation development and nuclear reprogramming. *Nat. Genet.*, **48**, 44–52.
  36. Wang, Y., Xu, Z., Jiang, J., Xu, C., Kang, J., Xiao, L., Wu, M., Xiong, J., Guo, X. and Liu, H. (2013) Endogenous miRNA sponge lincRNA-RoR regulates Oct4, Nanog, and Sox2 in human embryonic stem cell self-renewal. *Dev. Cell*, **25**, 69–80.
  37. Aubert, J., Stavridis, M.P., Tweedie, S., O'Reilly, M., Vierlinger, K., Li, M., Ghazal, P., Pratt, T., Mason, J.O., Roy, D. *et al.* (2003) Screening for mammalian neural genes via fluorescence-activated cell sorter purification of neural precursors from Sox1-gfp knock-in mice. *Proc. Natl Acad. Sci. U.S.A.*, **100**(Suppl. 1), 11836–11841.
  38. Sander, J.D., Maeder, M.L., Reyon, D., Voytas, D.F., Joung, J.K. and Dobbs, D. (2010) ZiFiT (Zinc Finger Targeter): an updated zinc finger engineering tool. *Nucleic Acids Res.*, **38**, W462–W468.
  39. Sander, J.D., Zaback, P., Joung, J.K., Voytas, D.F. and Dobbs, D. (2007) Zinc Finger Targeter (ZiFiT): an engineered zinc finger/target site design tool. *Nucleic Acids Res.*, **35**, W599–W605.
  40. Hwang, H.W., Wentzel, E.A. and Mendell, J.T. (2007) A hexanucleotide element directs microRNA nuclear import. *Science*, **315**, 97–100.
  41. Shevchenko, A., Tomas, H., Havlis, J., Olsen, J.V. and Mann, M. (2006) In-gel digestion for mass spectrometric characterization of proteins and proteomes. *Nat. Protoc.*, **1**, 2856–2860.
  42. Bartel, D.P. (2004) MicroRNAs: genomics, biogenesis, mechanism, and function. *Cell*, **116**, 281–297.
  43. Tan, J.Y., Sirey, T., Honti, F., Graham, B., Piovesan, A., Merkschlager, M., Webber, C., Ponting, C.P. and Marques, A.C. (2015) Extensive microRNA-mediated crosstalk between lincRNAs and mRNAs in mouse embryonic stem cells. *Genome Res.*, **25**, 655–666.
  44. Enright, A.J., John, B., Gaul, U., Tuschl, T., Sander, C. and Marks, D.S. (2003) MicroRNA targets in Drosophila. *Genome Biol.*, **5**, R1.
  45. Shyh-Chang, N. and Daley, G.Q. (2013) Lin28: primal regulator of growth and metabolism in stem cells. *Cell Stem Cell*, **12**, 395–406.
  46. Cimadamore, F., Amador-Arjona, A., Chen, C., Huang, C.T. and Terskikh, A.V. (2013) SOX2-LIN28/let-7 pathway regulates proliferation and neurogenesis in neural precursors. *Proc. Natl Acad. Sci. U.S.A.*, **110**, E3017–E3026.
  47. Ala, U., Karreth, F.A., Bosia, C., Pagnani, A., Taulli, R., Leopold, V., Tay, Y., Provero, P., Zecchina, R. and Pandolfi, P.P. (2013) Integrated transcriptional and competitive endogenous RNA networks are cross-regulated in permissive molecular environments. *Proc. Natl. Acad. Sci. U.S.A.*, **110**, 7154–7159.
  48. Bosia, C., Pagnani, A. and Zecchina, R. (2013) Modelling Competing Endogenous RNA Networks. *PLoS One*, **8**, e66609.
  49. Figliuzzi, M., Marinari, E. and De Martino, A. (2013) MicroRNAs as a selective channel of communication between competing RNAs: a steady-state theory. *Biophys. J.*, **104**, 1203–1213.
  50. Bujnicki, J.M., Feder, M., Radlinska, M. and Blumenthal, R.M. (2002) Structure prediction and phylogenetic analysis of a functionally diverse family of proteins homologous to the MT-A70 subunit of the human mRNA: m<sup>6</sup>A methyltransferase. *J. Mol. Evol.*, **55**, 431–444.
  51. Ebert, M.S., Neilson, J.R. and Sharp, P.A. (2007) MicroRNA sponges: competitive inhibitors of small RNAs in mammalian cells. *Nat. Methods*, **4**, 721–726.
  52. Wang, J., Cao, N., Yuan, M., Cui, H., Tang, Y., Qin, L., Huang, X., Shen, N. and Yang, H.T. (2012) MicroRNA-125b/Lin28 pathway contributes to the mesodermal fate decision of embryonic stem cells. *Stem Cells Dev.*, **21**, 1524–1537.
  53. Piskounova, E., Polytarchou, C., Thornton, J.E., LaPierre, R.J., Pothoulakis, C., Hagan, J.P., Iliopoulos, D. and Gregory, R.I. (2011) Lin28A and Lin28B inhibit let-7 microRNA biogenesis by distinct mechanisms. *Cell*, **147**, 1066–1079.
  54. Lee, S.H., Cho, S., Kim, M.S., Choi, K., Cho, J.Y., Gwak, H.S., Kim, Y.J., Yoo, H., Lee, S.H., Park, J.B. *et al.* (2014) The ubiquitin ligase human TRIM71 regulates let-7 microRNA biogenesis via modulation of Lin28B protein. *Biochim. Biophys. Acta*, **1839**, 374–386.
  55. Li, M.A., Amaral, P.P., Cheung, P., Bergmann, J.H., Kinoshita, M., Kalkan, T., Ralser, M., Robson, S., Meyenn, F.V., Paramor, M. *et al.* (2017) A lincRNA fine tunes the dynamics of a cell state transition involving Lin28, let-7 and de novo DNA methylation. *Elife*, **6**, e23468.
  56. Yang, Y., Fan, X., Mao, M., Song, X., Wu, P., Zhang, Y., Jin, Y., Yang, Y., Chen, L., Wang, Y. *et al.* (2017) Extensive translation of circular RNAs driven by N<sup>6</sup>-methyladenosine. *Cell Res.*, **27**, 626–641.
  57. Meyer, K.D., Saletore, Y., Zumbo, P., Elemento, O., Mason, C.E. and Jaffrey, S.R. (2012) Comprehensive analysis of mRNA methylation reveals enrichment in 3' UTRs and near stop codons. *Cell*, **149**, 1635–1646.

58. Dominissini, D., Moshitch-Moshkovitz, S., Schwartz, S., Salmon-Divon, M., Ungar, L., Osenberg, S., Cesarkas, K., Jacob-Hirsch, J., Amariglio, N., Kupiec, M. *et al.* (2012) Topology of the human and mouse m<sup>6</sup>A RNA methylomes revealed by m<sup>6</sup>A-seq. *Nature*, **485**, 201–206.
59. Liu, N., Dai, Q., Zheng, G., He, C., Parisien, M. and Pan, T. (2015) N<sup>6</sup>-methyladenosine-dependent RNA structural switches regulate RNA-protein interactions. *Nature*, **518**, 560–564.
60. Zhao, B.S. and He, C. (2015) Fate by RNA methylation: m<sup>6</sup>A steers stem cell pluripotency. *Genome Biol.*, **16**, 43.
61. Wang, Y., Li, Y., Toth, J.I., Petroski, M.D., Zhang, Z. and Zhao, J.C. (2014) N<sup>6</sup>-methyladenosine modification destabilizes developmental regulators in embryonic stem cells. *Nat. Cell Biol.*, **16**, 191–198.